



ELSEVIER

Available online at [www.sciencedirect.com](http://www.sciencedirect.com)

SCIENCE @ DIRECT®

C. R. Physique 4 (2003) 437–449



Exotic nuclei/Les noyaux exotiques

## Halo and skin nuclei

Isao Tanihata\*, Rituparna Kanungo

RIKEN, 2-1 Hirosawa, Wako, Saitama 351-0198, Japan

Presented by Guy Laval

### Abstract

The changes in nuclear structure far from the stability line are reviewed for light nuclei. The basic concepts of neutron and proton skins and neutron halos are presented with several experimental data. Signatures of new mode of collective excitation as consequences of such exotic structures are also shown. These changes of structure point to the need for the detailed study of single-particle orbitals for unstable nuclei. Such recent studies, in particular, the spectroscopic information of halo states, are reviewed. Changes of neutron orbital ordering away from the stability line are observed from such studies. Its most profound implication has emerged in the change of magic numbers. An over view of magic number variation is presented. *To cite this article: I. Tanihata, R. Kanungo, C. R. Physique 4 (2003).*

© 2003 Académie des sciences. Published by Éditions scientifiques et médicales Elsevier SAS. All rights reserved.

### Résumé

**Halos et peaux dans les noyaux atomiques.** Les modifications de la structure nucléaire loin de la stabilité sont passées en revue. Les concepts de Halos et de peaux de protons et de neutrons sont présentés en s'appuyant sur de nombreux résultats expérimentaux. Des signatures des nouveaux modes collectifs attendus comme conséquences de ces structures exotiques sont aussi décrites. Ces profondes transformations de la structure des noyaux démontrent la nécessité d'étudier les orbitales des nucléons dans les noyaux instables. Ces études récentes, en particulier en ce qui concerne les informations spectroscopiques pour les noyaux à halos, sont résumées. Une modification de l'ordre des orbitales de neutrons loin de la stabilité a été observée lors de ces études. L'implication la plus spectaculaire de cette transformation est la modification des nombres magiques. Une synthèse des résultats sur la modification de la magie est finalement présentée. *Pour citer cet article: I. Tanihata, R. Kanungo, C. R. Physique 4 (2003).*

© 2003 Académie des sciences. Published by Éditions scientifiques et médicales Elsevier SAS. All rights reserved.

### 1. Introduction

The nuclear density distribution is an important bulk property of nuclei that determines the nuclear potential, single-particle orbitals, and the wave function. Since the first use of RI beams, nucleon density distributions have been studied extensively for unstable nuclei. These studies opened up a new point of view on nuclear structure. Neutron skins and neutron halos are typical of such new structure. These new structures have introduced the decoupling of proton and neutron distributions and also related phenomena, such as soft mode of excitations.

Before the invention of RI beams, nuclear densities have been studied mainly by electron scattering and by proton scattering. Such studies, however, were restricted to stable nuclei as was the case in other nuclear reaction studies. From studies of stable nuclei, three 'basic properties' of nuclear density had been established:

\* Corresponding author.

E-mail address: [Tanihata@rarfaxp.riken.go.jp](mailto:Tanihata@rarfaxp.riken.go.jp) (I. Tanihata).

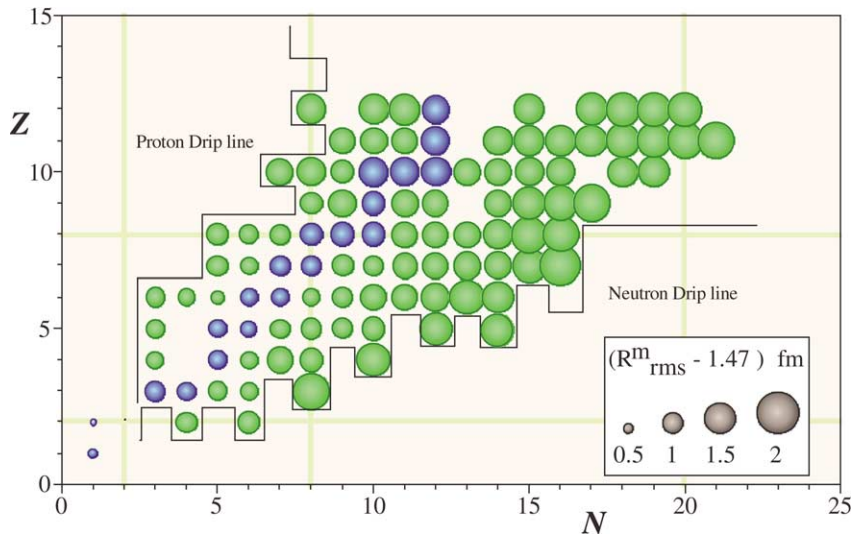


Fig. 1. Root-mean-square matter radii of light nuclei.

- (1) Half-density radius of the matter distribution is expressed as  $r_0 A^{1/3}$ , where  $r_0$  is the radius constant;
- (2) Protons and neutrons are homogeneously mixed in the nucleus, namely  $\rho_p(r) \propto \rho_n(r)$ ;
- (3) Surface thickness is constant.

For the determination of radii of unstable nuclei, isotope-shift measurements had been a unique technology. However, due to the limitation of accessible elements in ion source and of laser frequencies, such measurements have been made only for a limited number of elements. Moreover, these measurements provide only the information of charge radii or proton radii. The information was somehow remote to the study of the change of the nuclear size, because proton radii were studied by changing the neutron numbers. Almost no studies were made for the matter density distribution of unstable nuclei until the RI beam method was invented.

The production and use of RI beams, which has been started in the mid 1980s [1,2], broke this restriction and enabled the study of matter radii and matter density distributions of unstable nuclei extending up to the proton and neutron drip lines.

From the studies of matter distributions of unstable nuclei, it was found that the three ‘basic properties’ shown above are valid only for stable nuclei and do not hold for unstable nuclei. This fact is easily seen in the two-dimensional display of nuclear root-mean-square radii in nuclear chart as shown in Fig. 1. These rms radii of nucleon-distributions have been determined by the measurements of interaction cross sections using high-energy ( $\sim 800A$  MeV) RI beams [3,4]. The observed differences of the radii between isobars clearly show the break of ‘basic property 1’. A faster increase of Na isotope radii is the reflection of neutron skin, which will be discussed later, and indicates the breaking of ‘basic property 2’. The sudden large increase of the radii near the neutron drip line is the reflection of neutron halo and show the break of ‘basic property 3’.

Since the discovery and the explanation of magic numbers in nuclei by Mayers and Jensen, they have been a building block of nuclear models. In particular the nuclear shell model was developed tremendously into an accurate and useful theory. In nuclei far from the stability line, several indications of the disappearance of magic numbers have been reported. However, it was only after the study with RI beams that scientists seriously study the modification of magic numbers in nuclei far from the stability line. As discussed in detail later, it is found that all studied neutron magic numbers ( $N = 8, 20,$  and  $28$ ) disappears near the neutron drip line. Instead, evidence was found for new magic numbers such as  $N = 6, 16$  and others. Studies of shell structures and magic numbers are, therefore, hot topics of present day research.

In this paper, firstly basic concepts of these new structures are shown. Then recent studies related to skins and halos and their spectroscopic studies are reviewed in the following sections.

## 2. Nuclear skin

The first suggestion of a thick neutron skin was reported by Tanihata et al. [5] from a cluster-type model analysis of the interaction cross sections, two-neutron removal cross sections, and four-neutron removal cross section of  ${}^4, {}^6, {}^8\text{He}$ . Extremely thick neutron skin of about 0.8 fm was suggested in  ${}^8\text{He}$ . Recent proton elastic scattering studies of  ${}^6\text{He}$  and  ${}^8\text{He}$  by Egelhof et

al. [6] show more detailed density distributions and confirmed the neutron skin. The determined density distributions are shown in Fig. 2.

The first direct comparison between nuclear matter and charge radii over a wide range of neutron numbers was made in Na isotopes. Suzuki et al. [7] extracted the rms radii of proton and neutron distributions by combining the isotope shift and interaction cross-sections data. Fig. 3 shows the results of the analysis. The proton rms radii  $\langle r_p^2 \rangle^{1/2}$  and the neutron rms radii  $\langle r_n^2 \rangle^{1/2}$  are plotted as a function of the neutron number of the Na isotopes. In contrast to the slow change of  $\langle r_p^2 \rangle^{1/2}$ , neutron radius  $\langle r_n^2 \rangle^{1/2}$  increases monotonically as the neutron number increases. The thickness of the neutron skin  $\Delta R (= \langle r_n^2 \rangle^{1/2} - \langle r_p^2 \rangle^{1/2})$  increase up to 0.4 fm in the most neutron-rich Na isotope studied here. This value of neutron skin is much larger than a possible skin (0.12 fm) observed in the most neutron rich stable isotope  $^{48}\text{Ca}$ .

Other indirect evidence exists from Mg isotopes and for  $A = 20$  isobars [7,8]. Recent suggestive data are obtained by systematic measurements of charge changing cross sections ( $\sigma_{cc}$ ) of B to F isotopes [9]. As shown in Fig. 4 the charge changing

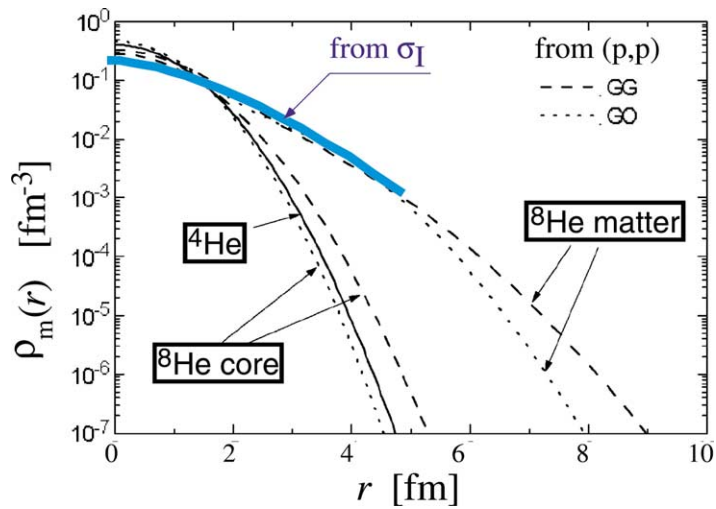


Fig. 2. Density distributions of  $^8\text{He}$  from two methods.

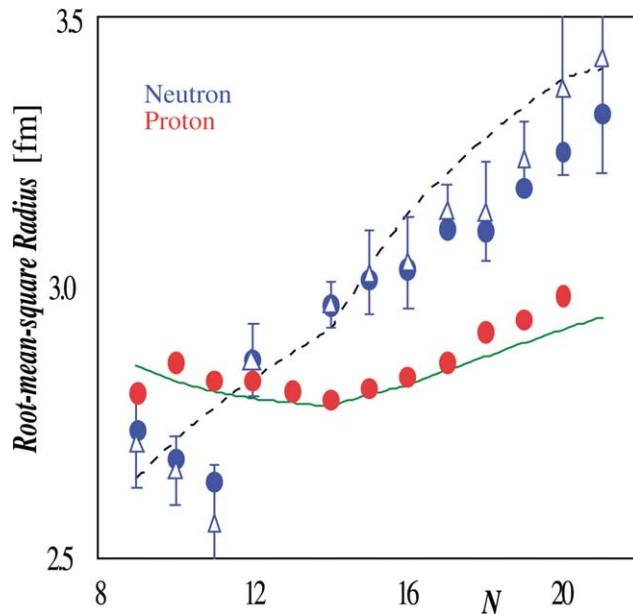


Fig. 3. Neutron and proton radii of Na isotopes. Neutron radii increase faster than that of protons and indicate the formation of neutron skin.

cross section does not increase when neutron number increases for a particular element. Instead, an increase is observed when proton number increases. At high-energies,  $\sigma_{cc}$  is directly related to charge distribution through the Glauber model analysis. A  $\sigma_{cc}$  may be larger than the estimation of the Glauber model due to possible proton emission at the ablation stage of the reaction. Therefore  $\sigma_{cc}$  provides an upper limit on the charge radius. A combination of  $\sigma_I$  and  $\sigma_{cc}$ , therefore, allows us to deduce the minimum estimation of the neutron skin thickness. Interaction cross sections increase monotonically when the neutron number increases for all elements. Therefore, the constancy of  $\sigma_{cc}$  for isotopes in Fig. 4 indicates the development of neutron skin in all elements shown there.

In Na isotope data (see Fig. 3), slightly larger radii of proton distribution are seen for most neutron deficient isotopes. This, therefore, suggests a proton skin of about 0.1 to 0.2 fm in these nuclei. The radii of proton and neutron distributions are same only for stable isotope  $^{23}\text{Na}$ .

The next light isotope chain with known charge radii is Ar. Recently,  $\sigma_I$  of neutron deficient Ar isotopes have been determined [10]. Proton skins are observed clearly.

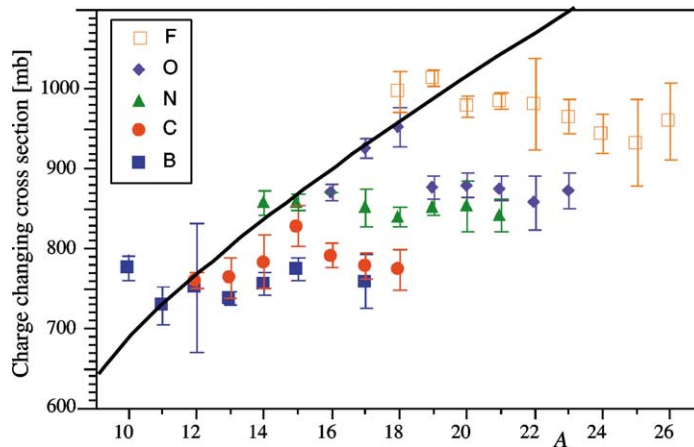


Fig. 4. Charge-changing cross sections with C target. The curve in the figure shows the  $A^{1/3}$  dependence of radii that is followed well for stable nuclei.

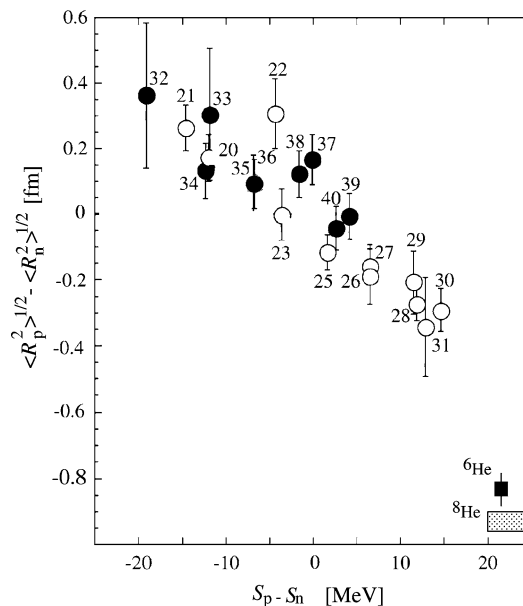


Fig. 5. Relation between the separation-energy difference and skin thickness.

From these data, it is considered that the neutron skin and proton skin are common phenomena in unstable nuclei. However, skins do not exist (or are extremely small if at all) in stable nuclei. Fig. 5 shows the difference of proton and neutron radii ( $\Delta R$ ) as a function of difference of proton and neutron separation energies  $\Delta S_{pn} = S_p - S_n$ . A strong linear correlation is seen between  $\Delta S_{pn}$  and  $\Delta R$ . It is also important to mention that the  $\Delta R$  is close to zero when  $\Delta S_{pn}$  is zero. The proportionality of proton and neutron densities thus seems to hold only for stable nuclei. Therefore it is considered that the difference in Fermi energies between proton and neutron is the relevant parameter for the neutron skin.

### 3. Nuclear halo

A low-density tail of neutron distribution (neutron halo) has been discovered from an abrupt increase of the interaction cross sections and a narrow momentum distribution of a neutron (or neutrons) in such a nucleus. The apparent reason of formation of neutron halo is the weak binding of the neutron. The asymptotic density tail of an s-wave neutron in the potential is described as

$$\rho(r) = |\Psi(r)|^2 = \left(\frac{2\pi}{\kappa}\right)^2 \left(\frac{e^{-2\kappa r}}{r^2}\right) \left[\frac{e^{2\kappa R}}{1 + \kappa R}\right], \tag{1}$$

where  $R$  is the width of the square well potential as an example. The parameter  $\kappa$ , which determines the slope of the density tail, is related to the neutron separation energy ( $S_n$ ) as,  $(\hbar\kappa)^2 = 2\mu S_n$ , where  $\mu$  is the effective mass of the system. As can be seen from these equations, the tail of the distribution becomes longer when  $S_n$  becomes smaller. However, in real situation, different orbitals contribute to the neutron wave function.

From analysis of the two-body halo wave function, Riisager et al. [11] found that s-wave and p-wave contribute to form single-neutron halo in a most drastic way. Similarly, from three-body analysis, it was found that  $K = 0, 1$  waves most strongly contribute to form two-neutron halo [12,13]. It is essentially due of the small centrifugal barrier for those neutrons. In fact, these analyses showed that the rms radii of these neutron distributions diverge when  $S_n$  or  $S_{2n}$  goes to 0. Instead, the rms radius of wave function with angular momentum larger than or equal to 2 (or  $K \geq 2$ ) remains at a finite value in the same limit. Recently, effects of the pairing interaction to the halo density were studied using the Hartree–Fock–Bogoliubov model. It was found that the tail of the density distribution would be reduced very much by the pairing of two neutrons in a halo. However, the observed large neutron tail in  $^{11}\text{Li}$  is not consistent with the conclusion of the model. It is then considered that the result of the Hartree–Fock–Bogoliubov model is only valid for heavier nuclei. In contrast to this, a relativistic-mean-field approach with pairing interaction predicts the giant halo in even neutron nuclei [14]. It is an interesting question whether a neutron halo exists or not in heavier nuclei.

The density distributions of halo nuclei have been determined by several methods. The best method is high-energy proton scatterings. In addition to the density distribution of He isotopes shown in Fig. 2, the density distribution of  $^{11}\text{Li}$  has been determined by proton elastic scattering at 800 MeV [6], as shown in Fig. 6. The long tail of the density distribution is clearly seen. This density distribution is consistent with the density distribution deduced from the interaction cross sections by the method shown below.

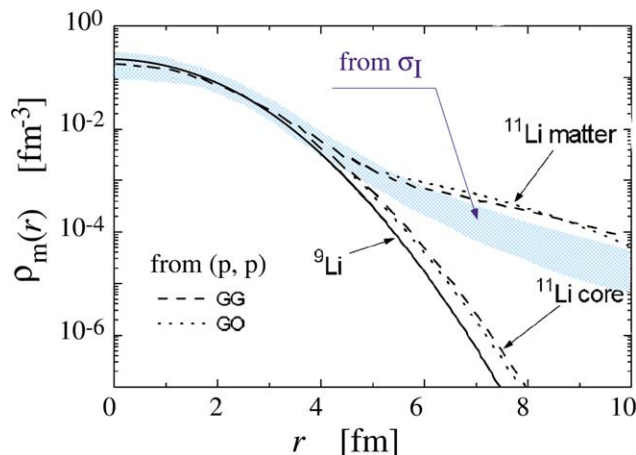


Fig. 6. Density distribution of  $^{11}\text{Li}$ . Black curves are density determined by proton scattering and the blue region shows the density determined by  $\sigma_I$ .

The density distributions of other neutron halo nuclei have not yet been determined by elastic scattering. Instead, careful analyses of interaction- and reaction-cross sections using model density distributions have been used to determine density distributions [3,4]. The sensitivity of the reaction cross section to the density tail can be changed either by changing the nucleon-nucleon cross section or by changing the target density distribution. The former corresponds to measurements of reaction cross sections at different energies, the latter corresponds to measurements with different targets. From these measurements density distributions have been determined and long tails in the density distributions were confirmed [15–17].

Another method for the determination of a density distribution assumes the relation between the asymptotic tail of the density distribution and the neutron separation energy to be single particle in nature. In this model, halo nuclei are assumed to have the (core + neutron) structure and the last neutron has a single-particle wave function in a Woods–Saxon potential. A few-body Glauber model [18] has been used for this analyses. Density distributions of many light neutron-rich nuclei have been determined and significant long tails of the neutron distribution have been observed from He to C isotopes as shown in [4].

Proton halos are also searched by the interaction and reaction cross sections. Possible evidences of long tails have been shown in  $^8\text{B}$ ,  $^{17}\text{Ne}$ ,  $^{23}\text{Al}$  [19,20]. However, there is not enough data to discuss the density distribution yet.

Recent interest in halo nuclei goes beyond matter distribution and is now focused on understanding the spectroscopic information of halo states. Such spectroscopic studies are presented in Section 5 below.

#### 4. Soft mode of excitation

The collective excitations of nuclei such as E1 giant resonance and Gamow–Teller resonance are specific oscillations in nuclei between protons and neutrons. The development of a skin and a halo adds new possible modes of collective excitation of nuclei. Because of the widening of the density distribution due to a skin and a halo, new modes of excitations are expected to appear at low energies and thus are called as soft modes. A collective E1-excitation is one such new mode. In a halo nucleus, neutrons in the halo are decoupled from those in the core of the nucleus. Therefore an oscillation of the relative position between the core and the halo is expected to appear. Because the density of the halo is extremely low, the frequency of such an oscillation is expected to be extremely low (within a few MeV) compared with the usual oscillation between protons and neutrons.

A soft dipole mode was suggested first by Hansen and Jonson as an enhancement of break up cross sections [21]. Then Ikeda generalized it to the collective oscillation at low energy, separated from the normal high-energy oscillation [22]. Experimentally, the large enhancements of the electromagnetic dissociation cross sections were discovered in  $^6\text{He}$  and  $^{11}\text{Li}$  [23].

Concerning the soft-dipole resonance, a  $1^-$  excited state at low energy in  $^6\text{He}$  was searched by  $^6\text{Li}(^7\text{Li}, ^7\text{Be})^6\text{He}$  reaction at 65A MeV. In addition to the known ground state and  $2^+$  first excited state and giant-dipole resonance at 8.5 MeV, Nakayama et al. observed a resonance at  $E_x = 4 \pm 1$  MeV and  $\Gamma = 4$  MeV of which  $\Delta S$ ,  $\Delta L$ ,  $E_x$  and  $\sigma$  are consistent with those values expected from the soft-dipole resonance [24].

In  $^{11}\text{Li}$ , a  $1^-$  excited state was observed firstly by Kobayashi et al. [25] by double-charge-exchange reaction,  $^{11}\text{B}(\pi^-, \pi^+)^{11}\text{Li}$ . They found a state at 1.2 MeV excitation energy and the angular distribution was consistent with the transition with  $\Delta L = 1$ . This level was also observed soon later by Korshennikov et al. [26,27] by the inelastic scattering of proton at 68 MeV. The excitation energy was  $E_x = 1.25 \pm 0.15$  MeV. The angular distribution of the inelastic scattering indicated the  $\Delta L = 1$  from the ground state. Right after this observation, Karataglidis et al. analyzed this data and presented the possibility that the observed angular distribution may be due to the shake-off mechanism, and may not be due to the resonance. However, recently, a study was made by the completely different type of reaction  $^{14}\text{C}(\pi^-, \text{pd})^{11}\text{Li}$  [28]. Three new excited states were observed at  $1.02 \pm 0.07$ ,  $2.07 \pm 0.12$ , and  $3.63 \pm 0.13$  MeV. The first one seems consistent with the state observed by the proton inelastic scattering and double charge exchange reaction. Moreover, recently a theoretical study also showed that the shake off mechanism fails to explain the proton elastic scattering data [29,30]. Therefore we consider that the existence of  $\Delta L = 1$ ,  $E_x = 1.2$  MeV is now confirmed.

Three electromagnetic dissociation experiments have been reported for  $^{11}\text{Li}$  [31–33]. Recent theoretical analyses of these data suggest the contribution from the continuum E1 excitation. However, it was seen that these three data are not consistent with each other, and thus it is not possible to discuss a resonant state [34]. Further careful experiments are definitely necessary in this direction.

Clear data for the evidence of continuum soft E1 mode of excitation was observed in  $^{11}\text{Be}$  [35]. It is also simple to understand the mechanism based on the transition to continuum because  $^{11}\text{Be}$  has a single-neutron halo. A direct break-up model calculation gives the E1 distribution as

$$\frac{dB(E1)}{dE_x} = S \left| \left\langle q \left| e \frac{Z}{A} r Y_m^1 \right| N_0 \sqrt{\frac{\kappa}{2\pi}} \frac{\exp(-\kappa r)}{r} \right\rangle \right|^2 \quad (2)$$

$$= S \frac{\exp(2\kappa r_0)}{1 + \kappa r_0} \frac{3\hbar^2}{\pi^2 \mu} e^2 \left( \frac{Z}{A} \right)^2 \frac{\sqrt{E_s} (E_x - E_s)^{3/2}}{E_x^4}. \quad (3)$$

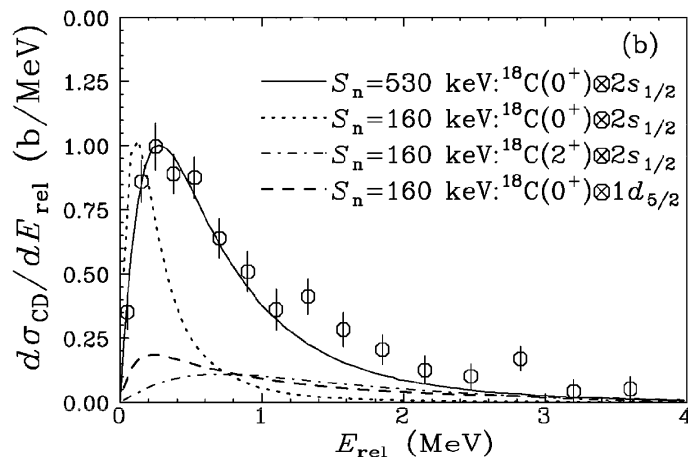


Fig. 7. Coulomb dissociation of  $^{19}\text{C}$ .  $E_{\text{rel}}$  is the relation energy between the fragment  $^{18}\text{C}$  and neutron. Best fit is obtained with  $s_{1/2}$  wave and using the neutron separation energy of 530 keV.

Here  $S$  is the spectroscopic factor of the  $2s_{1/2}$  state. Other variables:  $\kappa$  is defined by  $\kappa = \sqrt{2\mu E_s}/\hbar$ ,  $\mu$  is the reduced mass,  $E_s$  is the separation energy of neutron,  $E_x$  is the excitation energy, and  $r_0$  is the radius of the square-well potential relevant to the halo neutron. A good fit to the data shows the dominance of the non-resonant E1 transition of the halo neutron. The E1 nature of the transition was also confirmed by the angular distribution around the reaction plane of neutron emission in the EMD process. In  $^{11}\text{Be}$ , a strong E1 transition was observed to the bound first excited state [36] ( $E_x = 0.3198$  MeV,  $I^\pi = 1/2^-$ ) and thus it is reasonable that only the continuum contribution was observed in the dissociation process.

Coulomb dissociation has also been measured recently for  $^{19}\text{C}$ . The excitation spectrum is well explained by the non-resonant break up if the ground state spin  $1/2^+$  is assumed, as shown in Fig. 7, by the solid curve together with the data.

## 5. Spectroscopic information of halo nuclei

The quest for the ground state configuration of the unstable nuclei around the drip lines has gained importance not only for understanding the nuclear structure but it also provides knowledge on the change of single-particle levels far from stability. The tools for such spectroscopic information concerning nuclear ground state configurations maybe broadly classified into three categories. The first is the one or two nucleon transfer reaction, which have been the most reliable methods to determine the spectroscopic factors of nuclei. However, close to drip lines, due to very low beam intensity, such reactions often become too difficult to probe the structure. We thus, take recourse to reactions yielding larger cross sections. The second is fragmentation or ‘knockout’ reaction. The third is magnetic moment. Let us see, in some detail, such studies.

The most commonly used tool is the fragmentation or ‘knockout’ reaction, which has a relatively large one or two neutron (proton) removal cross sections. It has been shown [37] that the momentum distribution of projectile fragments reflects the motion of the nucleons inside the nucleus. Thus, to have information on the orbitals of the valence neutron in a nucleus  $^A\text{X}_N$ , one measures the longitudinal momentum distribution of the ‘core fragment’  $^{A-1}\text{X}_{N-1}$ . The presence of a halo structure is associated with the observation of a much narrower momentum distribution width compared to the Goladhaber [37] estimate for stable nuclei. Recently, this method has been made more complete by making measurements in coincidence with the core de-excitation gamma rays [38,39] (Fig. 8). This helps us to obtain knowledge of the fraction of core-excited component in the ground state configuration of nucleus  $^A\text{X}_N$ .

Generally, such measurements employ the use of a magnetic spectrometer, whereby one can identify the nucleus  $^{A-1}\text{X}_{N-1}$  and determine its momentum from magnetic rigidity analysis. This technique has been used worldwide in various laboratories such as MSU, GSI, GANIL and RIKEN. A new experimental method has recently been developed at RIKEN [40] which is based on the derivation of momentum from a time-of-flight of the fragments, without the use of a bending magnet. A unique and advantageous feature is its wide angular momentum acceptance, which allows measurements of a variety of fragments simultaneously.

However, one often wonders about the distortion effects due to different reaction mechanisms from such fragmentation studies. As an alternative, the magnetic moment is a decisive tool to determine the ground state spin. The spin of  $^{17}\text{C}$  is a good example to show the usefulness of this method [41]. Suzuki et al. [42], suggested that magnetic moments would also be very sensitive to determine the mixing amplitude of different orbitals in the ground state.

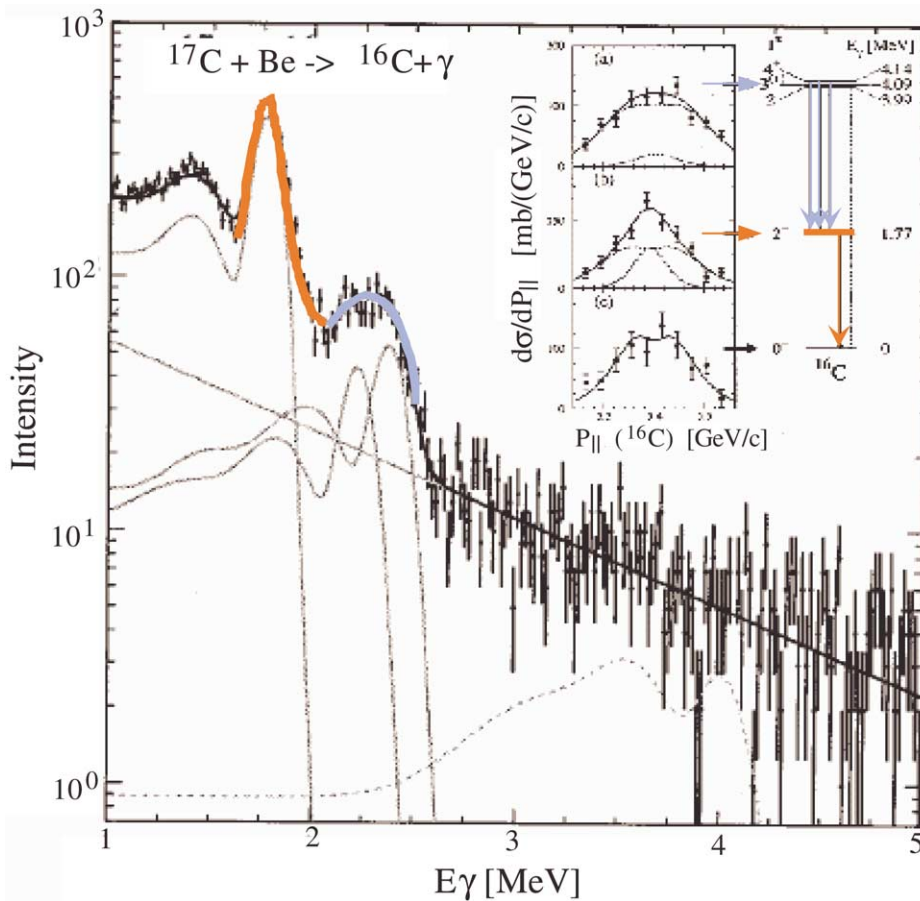


Fig. 8. Momentum distribution of  $^{17}\text{C}$  (inset) with gamma-ray coincidence with core fragment  $^{16}\text{C}$ .

In the following, we discuss spectroscopic information for neutron-rich nuclei in the p-sd shell that has been derived from the above discussed measurements. In a core + neutron model, in such regions, the ground state configuration can be expressed as a superposition of different core excited states, i.e.,  $\sum_{i=1}^n C_i \psi_c^i \cdot \phi_n^i$  where  $\psi_c^i$  is the wavefunction of the core in the  $i$ -th state coupled to a neutron,  $\phi_n^i$ , in  $2s_{1/2}$ ,  $1d_{5/2}$  or other relevant orbitals. Without the knowledge of the transition densities we approximate the excited core states to have the same density (wavefunction) as the ground state. The coefficients  $C_i$  give the fractional parentage of the  $i$ -th configuration with,  $\sum_{i=1}^n |C_i|^2 = 1$ . It should be noted that these values are different from the many-body spectroscopic factor ( $C^2 S_{ij}$ ). The spectroscopic factors and/or fractional parentages for the different configurations for some p-sd shell nuclei are listed in Table 1.

The lightest element that extends into the sd-shell is Beryllium.  $^{11}\text{Be}$  was the first one-neutron halo nucleus, having an abnormal ground state spin of  $1/2^+$ , instead of  $1/2^-$ . It is thus an interesting investigation ground due to the dramatic change of single particle levels causing a parity inversion between the  $2s_{1/2}$  and the  $1p_{1/2}$  orbitals.

The recently observed magnetic moment of  $^{11}\text{Be}$  [43], strongly required a large s-wave component in the wavefunction for its explanation. Such a parentage ( $C_i$ ) was confirmed by  $^{11}\text{Be}(p, d)^{10}\text{Be}$  transfer reaction [44,45], where only 16%  $d_{5/2}$  component was found to be present in the ground state of this nucleus. However, this strength was found to crucially depend on the type of model employed. A further confirmation in this respect can be found in the momentum distribution with and without gamma rays in coincidence [46,47].

The addition of one more neutron changed the scenario in  $^{12}\text{Be}$ , where, the momentum distribution from one neutron removal [48] conclusively demonstrated a nearly equal mixing of s- and d-waves leading to an s-wave spectroscopic factors ( $C^2 S_{ij}$ ) of  $0.42 \pm 0.06$ . Although, the above discussed reaction studies have not yet been extended to  $^{14}\text{Be}$ , again a strong s-wave component in this nucleus was suggested by other studies [49].

The next chain of odd Z, Boron isotopes, also shows interesting systematics, with the momentum distribution of  $^{14}\text{B}$  exhibiting a narrow width [50], showing the spectroscopic factor for the s-wave component coupled to core ground state to be



Table 1  
Spectroscopic factors and fractional parentage of halo states

Nucleus	$J^\pi$ of core	$E_x$ of core	$l$	$S$ -factor ( $S_{ij}$ )	Parentage ( $C_i$ )	Ref.
$^{11}\text{Be}$	$0^+$	0.0	0	0.74		[47]
	$2^+$	3.3	2	0.18		[47]
	$0^+$	0.0	0	0.66–0.79		[82]
	$2^+$	3.3	2	0.17–0.38		[82]
	$0^+$	0.0	0	0.76–1.1		[55]
$^{12}\text{Be}$	$1/2^+$	0.0	0			
	$1/2^-$	0.320	2			
$^{14}\text{B}$	$3/2^-$	0.0	2	0.31		[50]
			0	0.64		[50]
$^{17}\text{B}$	$3/2^-$	0.0	0		$0.69 \pm 0.20$	[52]
			2		$0.31 \pm 0.20$	[52]
$^{15}\text{C}$	$0^+$	0.0	0	0.65–1.03		[55]
	$2^+$	7.102	2	$0.10 \pm 0.03$		[55]
	$0^+$	0.0	0	0.83		[50]
$^{17}\text{C}$	$0^+$	0.0	2	0.03	$0.19 \pm 0.09$	[39]
			0	0.16	$0.14 \pm 0.06$	[39]
			2	1.44	$0.38 \pm 0.08$	[39]
	$2,3^{(+)}, 4^+$	4.1	0	0.22	$0.02 \pm 0.02$	[39]
			2	0.76	$0.27 \pm 0.05$	[39]
	$0^+$	0.0	2	0.035		[50]
	$2^+$	1.77	2	1.41		[50]
		0	0.16		[50]	
$^{19}\text{C}$	$0^+$	0.0	0	0.58	$0.56 \pm 0.09$	[39]
	$2^+$	1.6	2	0.48		[39]
	$2^+, 3^+$	4.9	2	2.44	$0.44 \pm 0.11$	[39]

0.64. An inclusive momentum distribution measurement [51], of two neutron removal momentum distribution of  $^{17}\text{B}$  suggests an s-wave strength of  $0.69 \pm 0.20$  in  $^{17}\text{B}$ , which is also consistent with a description of its large two-neutron removal cross section. Less is known about the most neutron rich boron isotope,  $^{19}\text{B}$  ( $S_{2n} = 0.5 \pm 0.4$  MeV). The interaction cross section measurement [52] suggests a large root-mean-square radius of  $3.11 \pm 0.13$  fm and the possibility of a core-plus-four neutron structure for this nucleus, similar to that of  $^8\text{He}$ .

Since the early 1970s Goss et al. [53] pointed out an abnormal spin of  $1/2^+$  of the ground state of  $^{15}\text{C}$  from (d, p) reactions and a large s-wave parentage of 80% in its ground state. Spectroscopic studies through momentum distribution measurements [54,55] confirmed this, although the value of the spectroscopic factor ( $C^2 S_{ij}$ ) was found to depend on the wave function and potential used. Magnetic moment studies [56] are not inconsistent with the large s-wave parentage.

Reaching out to more a neutron rich domain, the ground state spin of the  $^{17}\text{C}$  nucleus was found to be  $3/2^+$  from momentum-distribution measurements [39,57], which shows the importance of the  $2^+$  excited core of  $^{16}\text{C}$  in  $^{17}\text{C}$ . This was clearly confirmed by recent magnetic moment measurements [41] which exhibited a g-factor much smaller than the Schmidt value for a  $J^\pi = 1/2^+$  state.

The situation is a bit more complicated with the  $^{19}\text{C}$  nucleus whose spin is yet to be ascertained by magnetic moment measurements or some other method. Recent shell model predictions suggest a  $1/2^+$  ground state with very closely lying  $5/2^+$  and  $3/2^+$  excited states [58]. Momentum distribution measurements [57], however, show a moderately narrow width with an extended tail. Analysis by a core-plus-neutron Glauber model shows that a ground state of  $3/2^+$  and  $5/2^+$  give an overall better reproduction of the shape of the momentum distribution [59], but have too small cross sections. A later measurement detecting core de-excitation gamma rays [39] suggest that  $56 \pm 9\%$  of the configuration is associated with a ground state core coupled to an  $2s_{1/2}$  neutron giving  $1/2^+$  ground state. The interaction cross section [60] and Coulomb dissociation also points to a similar conclusion, but this configuration is not suitable for explaining the wide momentum tail. The situation is thus shrouded in controversy and no conclusion has yet been reached.

Moving to the Oxygen isotopes, an interesting anomaly appears for  $^{23}\text{O}$  showing an extremely large interaction cross section which is under predicted even with a 100% s-wave parentage [61,62] in a core-plus-neutron halo model. Therefore, it is considered that a new type of structure has to be introduced.

As a general scenario, the spectroscopy of neutron rich nuclei has revealed that ground state configurations of the p-sd shell nuclei show interesting deviations from a conventional shell model description as presented in Fig. 9. The lowering of the  $2s_{1/2}$  orbital occurs for nuclei with small separation energy thus favoring the formation of neutron halo. But at the same time

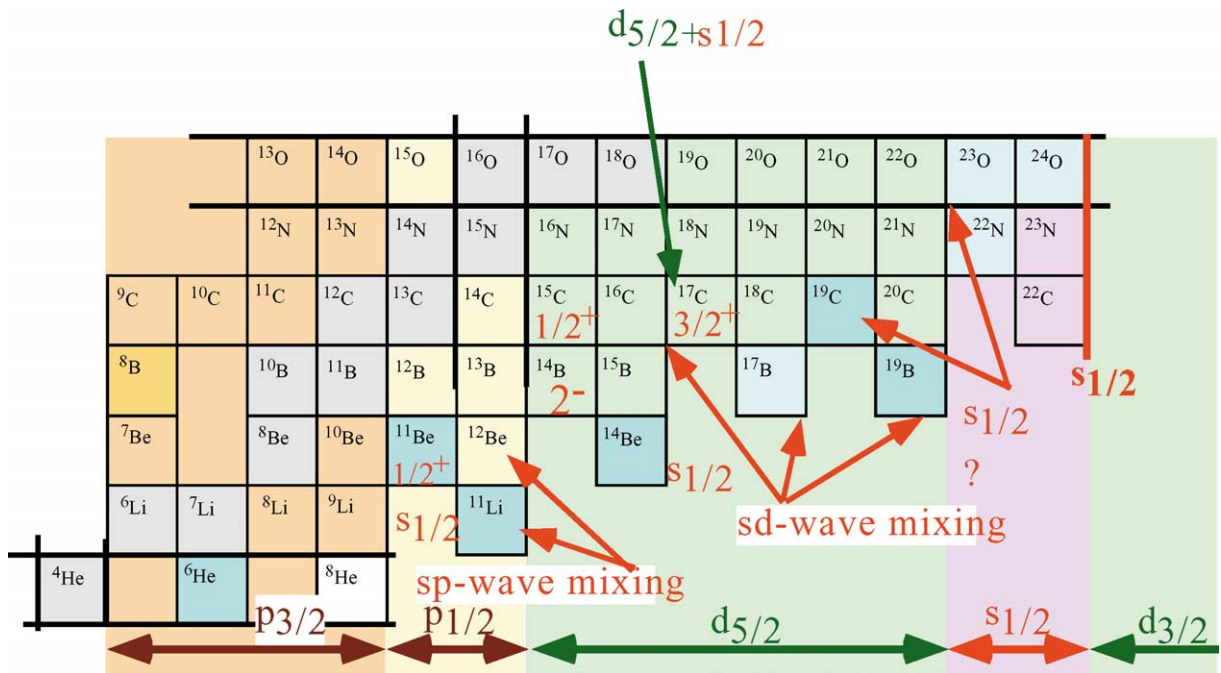


Fig. 9. Nuclear orbitals in p-sd shell nuclei. Horizontal arrows indicate the conventional shells and red characters shows the observed shells.

$2s_{1/2}$  and  $1d_{5/2}$  orbitals become very close and thus strong mixing occurs. A decrease of s-wave strength in the ground state configuration between  $^{11}\text{Be}$  and  $^{12}\text{Be}$  can be attributed to an effect of neutron pairing. Thus it appears that in s-d shell nuclei there should be a competitive process between weak binding and pairing to determine the relative contributions of the s and d orbitals.

## 6. Magic numbers

As a consequence of such changes in nuclear orbitals, it is naturally expected that the nuclear shell gaps would be modified in neutron- and proton-rich regions. The nucleon magic numbers can be identified from empirical systematics related to nuclear binding, such as, one-nucleon separation energy and beta-decay  $Q$ -values along the same isospin chain, avoiding pairing fluctuations, as discussed recently in [61,63]. A difference of two-neutron separation energies is also discussed as a possible signature [64]. The systematics of excitation energy ( $E_x(2^+)$ ) and  $B(E2)$  values of the even-even isotopes for neutron and proton rich nuclei also provide a good confirmation of magicity. Furthermore, the spectroscopy of nuclei, show the presence of intruder orbitals that signifies the breakdown of a shell closure.

The disappearance of the  $N = 8$  shell closure appeared as the first evidence in the discovery of the neutron halo in  $^{11}\text{Li}$  [2]. It showed the strong influence of the  $2s_{1/2}$  orbital in the supposedly  $p_{1/2}$  closed shell. It is now established by the confirmation of parity mixing in the ground state of  $^{11}\text{Li}$  [65]. The extension of this breakdown continues to Be isotopes, which can be observed clearly by the decrease in excitation energy of the  $2^+$  state from  $^{10}\text{Be}$  to  $^{12}\text{Be}$  associated with quadrupole collectivity and furthermore confirmed by the presence of a low lying  $1^-$  state [66]. Another confirmation of this comes from knockout studies of  $^{12}\text{Be}$ , which shows considerable s and d admixture in its ground state [48].

In addition to the anomaly of magnetic moment in Na isotopes [67], a large quadrupole collectivity observed for  $^{32}\text{Mg}$  confirmed breakdown of  $N = 20$  shell closure [68,69]. Studies of beta delayed neutron emission probabilities of  $^{44}\text{S}$  [70] suggest the weakening of  $N = 28$  shell closure in regions below  $^{48}\text{Ca}$ , but it persists in Ar isotopes [71]. Breakdown of  $N = 28$  shell closure has also been discussed in mean-field studies [72] predicting shape co-existence for  $^{44}\text{S}$ . The empirical systematic studies [63] also show clear indications for disappearance of  $N = 20, 28$  magic numbers.

Several theoretical studies have also suggested strong modification of shell closures far from stability [73,74] and it was a question whether shell structure may be dissolved in regions far from stability. However, recent studies of neutron separation energies and radii of C, N, O isotopes by Ozawa et al. have shown an appearance of a new magic number  $N = 16$  [61].

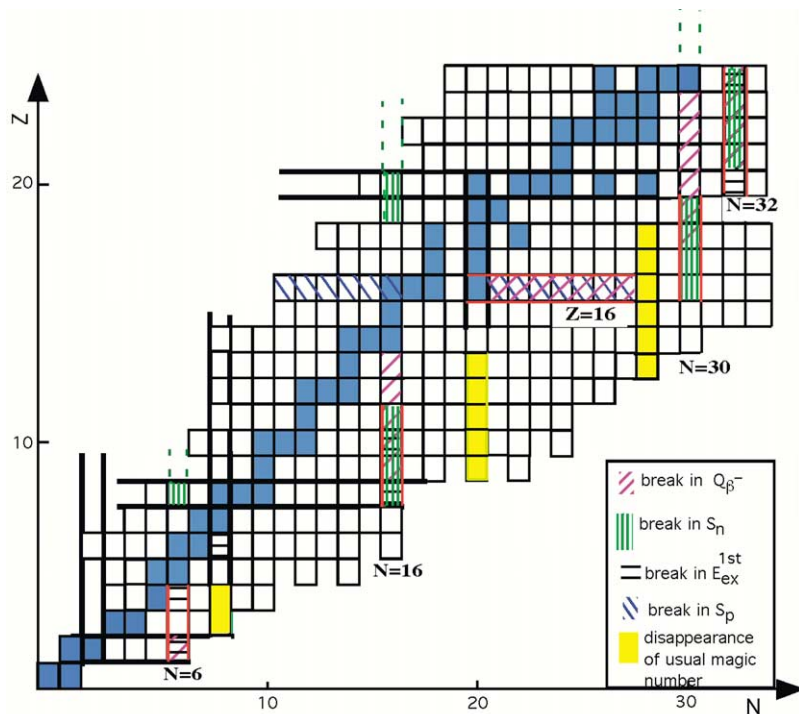


Fig. 10. Summary of change of magic numbers for light nuclei.

Further confirmation of this was found from an extensive study of other relevant quantities by Kanungo et al. [63], which also shows new regions of shell closures at  $N = 6, 30, 32$  in neutron rich nuclei. Interestingly  $Z = 16$  also shows a magic number behavior in neutron rich regions. Extending the same study to the proton rich part of the nuclear chart they find new shell gaps originating at proton number  $Z = 16$ , and  $N = 6, 16$  which are similar to the neutron rich side. This suggests a kind of mirror symmetry for the new shell gaps at either sides of the stability line. The  $N = 32$  sub-shell closure was also confirmed recently by the observation of a decrease in excitation energy of the  $2^+$  state from  $^{56}\text{Cr}$  to  $^{58}\text{Cr}$  [75].

The  $N = 16$  magic number was understood to originate due to a lowering of the  $2s_{1/2}$  orbital in regions of small separation energy [61]. The reason for  $N = 30$  and  $Z = 16$  magicity in neutron rich nuclei is yet to be understood. The  $N = 32$  shell gap may arise due to a lowering of the  $2p_{3/2}$  orbital [63] and has also been discussed to originate from diminished  $\pi 1f_{7/2}-\nu 1f_{5/2}$  monopole proton–neutron interaction [75].

Recently, Otsuka et al. [76] demonstrated the importance of the spin-isospin part of the nucleon–nucleon interaction in explaining both the disappearance of usual magic numbers ( $N = 20$ ) and the appearance of new ones at  $N = 6, 16, 34$  for beta unstable nuclei. While  $N = 6, 16$  have been confirmed from experimental studies [61,63], the latter still remains to be confirmed. Furthermore, this theory predicts the occurrence of similar shell closures for proton rich nuclei due to isospin symmetry which is in consonance to the observations of Kanungo et al. [63].

An alternative mechanism is proposed in [77] which demonstrates particle–vibration coupling to cause a large energy gap between  $2s_{1/2}$  and  $1d_{3/2}$  states leading to  $N = 16$  gap and likewise a reduced gap between the  $2s_{1/2}$  and  $1p_{1/2}$  states giving rise to shell quenching at  $N = 8$ . Changes of shell closures are also discussed in [78–80]. Sub-shell closure at  $N = 40$  is shown [81], based on particle–core coupling.

Fig. 10 summarizes the changes of shell closures for light nuclei [63]. However, for light nuclei, conventional doubly magic nuclei like  $^{10}\text{He}$ ,  $^{28}\text{O}$  are unbound. It is interesting to note that the existence of doubly magic  $^{78}\text{Ni}$ ,  $^{100,132}\text{Sn}$  may show the persistence of  $N = 50, 82$  shell closure there. The changes in shell closures in this area are important subjects of investigation as they are intricately related to the understanding of the r-process nucleosynthesis.

## 7. Summary

We have reviewed the studies of halo and skin of the nuclei. These features provide new viewpoints of nuclear structure. These are phenomena that occur in nuclei far from the stability line because of the smaller binding of neutrons in neutron-rich

nuclei or of protons in neutron-deficient nuclei due to the large asymmetry of proton and neutron numbers. In contrast, protons in neutron-rich nuclei (or neutrons in proton-rich nuclei) are much more strongly bound than those in stable nuclei. No studies have so far been made to look for the effect of this stronger binding. It might be an interesting new direction of study in unstable nuclei.

In the region far from the stability line, magic numbers are modified by many reasons. Classical magic numbers 8, 20, 28 have been observed to disappear in neutron-rich nuclei. Instead evidence of several new magic numbers appear for  $N = 6, 16, 32,$  and  $34$ . It is important to know how such a tendency would continue to heavier nuclei. In heavier nuclei, magic numbers in neutron-rich region are not only important for understanding nuclear structure, but also important for understanding nucleosynthesis in stars.

Studies of halo and skin have not only opened new opportunities in nuclear structure physics, but also have shown the necessity for further development of nuclear theory that works in the whole region of nuclei. Studies of nuclei far from the stability are thus considered to be one of the most important directions of physics in the present time.

## References

- [1] I. Tanihata, *Hyperfine Interactions* 21 (1985) 251.
- [2] I. Tanihata, H. Hamagaki, O. Hashimoto, et al., *Phys. Lett. B* 160 (1985) 380.
- [3] A. Ozawa, O. Bochkarev, L. Chulkov, et al., *Nucl. Phys. A* 691 (2001) 599.
- [4] A. Ozawa, T. Suzuki, I. Tanihata, *Nucl. Phys. A* 693 (2001) 32.
- [5] I. Tanihata, D. Hirata, T. Kobayashi, et al., *Phys. Lett. B* 289 (1992) 261.
- [6] P. Egelhof, G.D. Alkhazov, M.N. Andronenko, et al., *Eur. Phys. J. A* 15 (2002) 27.
- [7] T. Suzuki, H. Geissel, O. Bochkarev, et al., *Phys. Rev. Lett.* 75 (1995) 3241.
- [8] L. Chulkov, G. Kraus, O. Bochkarev, et al., *Nucl. Phys. A* 603 (1996) 219.
- [9] L.V. Chulkov, O.V. Bochkarev, D. Cortina-Gill, et al., *Nucl. Phys. A* 674 (2000) 330.
- [10] A. Ozawa, T. Baumann, L. Chulkov, et al., *Nucl. Phys. A* 709 (2002) 60.
- [11] K. Riisager, A.S. Jensen, P. Möller, *Nucl. Phys. A* 548 (1992) 393.
- [12] D.V. Fedorov, A.S. Jensen, K. Riisager, *Phys. Rev. C* 1994 (1994) 201.
- [13] D.V. Fedorov, A.S. Jensen, K. Riisager, *Phys. Rev. C* 50 (1994) 2372.
- [14] J. Meng, P. Ring, *Phys. Rev. Lett.* 80 (1998) 460.
- [15] M. Fukuda, T. Ichihara, N. Inabe, et al., *Phys. Lett. B* 268 (1991) 339.
- [16] I. Tanihata, T. Kobayashi, T. Suzuki, et al., *Phys. Lett. B* 287 (1992) 307.
- [17] T. Zheng, T. Yamauchi, A. Ozawa, et al., *Nucl. Phys. A* 709 (2002) 103.
- [18] Y. Ogawa, K. Yabana, Y. Suzuki, *Nucl. Phys. A* 543 (1992) 722.
- [19] A. Ozawa, T. Kobayashi, H. Sato, et al., *Phys. Lett. B* 334 (1994) 18.
- [20] X.Z. Cai, H.Y. Zhang, W.Q. Shen, et al., *Phys. Rev. C* 65 (2002) 024610.
- [21] P.G. Hansen, B. Jonson, *Europhys. Lett.* 4 (1987) 409.
- [22] K. Ikeda, *Nucl. Phys. A* 538 (1992) 355c.
- [23] T. Kobayashi, S. Shimoura, I. Tanihata, et al., *Phys. Lett. B* 232 (1989) 51.
- [24] S. Nakayama, T. Yamagata, H. Akimune, et al., *Phys. Rev. Lett.* 85 (2000) 262.
- [25] T. Kobayashi, *Nucl. Phys. A* 538 (1992) 343c.
- [26] A.A. Korshennikov, E.Y. Nikolskii, T. Kobayashi, et al., *Phys. Rev. C* 53 (1996) R537.
- [27] A.A. Korshennikov, E.A. Kuzmin, E.Y. Nikolskii, et al., *Phys. Rev. Lett.* 78 (1997) 2317.
- [28] M.G. Gornov, Y. Gurov, S. Lapushkin, et al., *Phys. Rev. Lett.* 81 (1998) 4325.
- [29] R. Crespo, I.J. Thompson, A.A. Korshennikov, *Phys. Rev. C* 66 (2002) 021002(R).
- [30] R. Crespo, I.J. Thompson, *Nucl. Phys. A* 689 (2001) 559.
- [31] D. Sackett, K. Ieki, A. Galonsky, et al., *Phys. Rev. C* 48 (1993) 118.
- [32] S. Shimoura, T. Nakamura, M. Ishihara, et al., *Phys. Lett. B* 348 (1995) 29.
- [33] M. Zinser, F. Humbert, T. Nilsson, et al., *Nucl. Phys. A* 619 (1997) 151.
- [34] C. Forssén, V.D. Efros, M.V. Zhukov, *Nucl. Phys. A* 706 (2002) 48.
- [35] T. Nakamura, S. Shimoura, T. Kobayashi, et al., *Phys. Lett. B* 331 (1994) 296.
- [36] D.J. Millener, J.W. Olness, E.K. Warburton, et al., *Phys. Rev. C* 28 (1983) 497.
- [37] A.S. Goldhaber, *Phys. Lett. B* 53 (1974) 306.
- [38] A. Navin, D. Bazin, B.A. Brown, et al., *Phys. Rev. Lett.* 81 (1998) 5089.
- [39] V. Maddalena, T. Aumann, D. Bazin, et al., *Phys. Rev. C* 63 (2001) 024613.
- [40] R. Kanungo, M. Chiba, N. Iwasa, et al., *Phys. Rev. Lett.* 88 (2002) 142502.
- [41] H. Ogawa, K. Asahi, H. Ueno, et al., *Eur. Phys. J. A* 13 (2002) 81.
- [42] T. Suzuki, T. Otsuka, A. Muta, *Phys. Lett. B* 364 (1995) 69.
- [43] W. Geithner, S. Kappertz, M. Keim, et al., *Phys. Rev. Lett.* 83 (1999).
- [44] S. Fortier, S. Pita, J.S. Winfield, et al., *Phys. Lett. B* 461 (1999) 22.

- [45] J.S. Winfield, S. Fortier, W.N. Catford, et al., Nucl. Phys. A 683 (2001) 48.
- [46] F. Negoita, C. Borcea, F. Carstoiu, et al., Phys. Rev. C 59 (1999) 2082.
- [47] T. Aumann, A. Navin, D.P. Balamuth, et al., Phys. Rev. Lett. 84 (2000) 35.
- [48] A. Navin, D.W. Anthony, T. Aumann, et al., Phys. Rev. Lett. 85 (2000) 266.
- [49] M. Labiche, N.A. Orr, F.M. Marqués, et al., Phys. Rev. Lett. 86 (2001) 600.
- [50] E. Sauvan, F. Carstoiu, N.A. Orr, et al., Phys. Lett. B 491 (2000) 1.
- [51] T. Suzuki, Y. Ogawa, M. Chiba, et al., Phys. Rev. Lett. 89 (2002) 012501.
- [52] T. Suzuki, R. Kanungo, O. Bochkarev, et al., Nucl. Phys. A 658 (1999) 313.
- [53] J.D. Goss, P.L. Jolivet, C.P. Browne, et al., Phys. Rev. C 12 (1975) 1730.
- [54] D. Bazin, W. Benenson, B.A. Brown, et al., Phys. Rev. C 57 (1998) 2156.
- [55] J.A. Tostevin, D. Bazin, B.A. Brown, et al., Phys. Rev. C 66 (2002) 024607.
- [56] K. Asahi, K. Sakai, H. Ogawa, et al., Nucl. Phys. A 704 (2002) 88c.
- [57] T. Baumann, M.J.G. Borge, H. Geissel, et al., Phys. Lett. B 439 (1998) 256.
- [58] B.A. Brown, B.H. Wildenthal, Ann. Rev. Nucl. Part. Sci. 38 (1988) 29.
- [59] R. Kanungo, I. Tanihata, Y. Ogawa, et al., Nucl. Phys. A 677 (2000) 171.
- [60] A. Ozawa, O. Bochkarev, L. Chulkov, et al., RIKEN-AF-NP-294 (1998).
- [61] A. Ozawa, T. Kobayashi, T. Suzuki, et al., Phys. Rev. Lett. 84 (2000) 5493.
- [62] R. Kanungo, I. Tanihata, A. Ozawa, Phys. Lett. B 512 (2001) 261.
- [63] R. Kanungo, I. Tanihata, A. Ozawa, Phys. Lett. B 528 (2002) 58.
- [64] H. Grawe, M. Lewitowicz, Nucl. Phys. A 693 (2001) 116.
- [65] H. Simon, D. Aleksandrov, T. Aumann, et al., Phys. Rev. Lett. 83 (1999) 496.
- [66] H. Iwasaki, T. Motobayashi, H. Akiyoshi, et al., Eur. Phys. J. 13 (2002) 55.
- [67] G. Huber, F. Touchard, S. Büttgenbach, et al., Phys. Rev. C 18 (1978) 2342.
- [68] T. Motobayashi, Y. Ikeda, Y. Ando, et al., Phys. Lett. B 346 (1995) 9.
- [69] D. Guillemaud-Mueller, C. Detraz, M. Langevin, et al., Nucl. Phys. A 426 (1984) 37.
- [70] O. Sorlin, D. Guillemaud-Mueller, A.C. Mueller, et al., Phys. Rev. C 47 (1993) 2941.
- [71] H. Scheit, T. Glasmacher, B.A. Brown, et al., Phys. Rev. Lett. 77 (1996) 3967.
- [72] T.R. Werner, J.A. Sheikh, W. Nazarewicz, et al., Phys. Lett. B 335 (1994) 259.
- [73] J. Dobaczewski, I. Hamamoto, W. Nazarewicz, et al., Phys. Rev. Lett. 72 (1994) 981.
- [74] R.C. Nayak, Phys. Rev. C 60 (1999) 064305.
- [75] J.I. Prisciandaro, P.F. Mantica, B.A. Brown, et al., Phys. Lett. B 510 (2001) 17.
- [76] T. Otsuka, R. Fujimoto, Y. Utsuno, et al., Phys. Rev. Lett. 87 (2001) 082502.
- [77] G. Colò, T. Suzuki, H. Sagawa, Nucl. Phys. A 695 (2001) 167.
- [78] Z. Dlouhy, J.C. Angélique, R. Anne, et al., Nucl. Phys. A 701 (2002) 189.
- [79] C. Samanta, S. Adhikari, Phys. Rev. C 65 (2002) 037301.
- [80] F. Sarazin, H. Savajols, W. Mittig, et al., Phys. Rev. Lett. 84 (2000) 5062.
- [81] A.M. Oros-Peusquens, P.F. Mantica, Nucl. Phys. A 669 (2000) 81.
- [82] S. Fortier, S. Pita, J.S. Winfield, et al., Phys. Lett. B 461 (1999) 22.